Published in final edited form as:
Nucl Med Biol. 2011 January ; 38(1): 53–62. doi:10.1016/j.nucmedbio.2010.07.005.

Synthesis, uptake mechanism characterization and biological evaluation of ^{18}F labeled fluoroalkyl phenylalanine analogs as potential PET imaging agents

Limin Wang[a], **Wenchao Qu**[b], **Brian P. Lieberman**[b], **Karl Plössl**[b], and **Hank F. Kung**[b,c,*]

[a] Department of Chemistry, University of Pennsylvania, Philadelphia, PA 19104, USA

[b] Department of Radiology, University of Pennsylvania, Philadelphia, PA 19104, USA

[c] Department of Pharmacology, University of Pennsylvania, Philadelphia, PA 19104, USA

Abstract

Introduction—Amino acids based tracers represent a promising class of tumor metabolic imaging agents with successful clinical applications. Two new phenylalanine derivatives, *p*-(2-[^{18}F]fluoroethyl)-L-phenylalanine (FEP, [^{18}F]**2**) and *p*-(3-[^{18}F]fluoropropyl)-L-phenylalanine (FPP, [^{18}F]**3**) were synthesized and evaluated in comparison to clinically utilized *O*-(2-[^{18}F]fluoroethyl)-L-tyrosine (FET, [^{18}F]**1**).

Methods—FEP ([^{18}F]**2**) and FPP ([^{18}F]**3**) were successfully synthesized by a rapid and efficient two-step nucleophilic fluorination of tosylate precursors and deprotection reaction. In vitro cell uptake studies were carried out in 9L glioma cells. In vivo studies, 9L tumor xenografts were implanted in Fisher 344 rats.

Results—FEP ([^{18}F]**2**) and FPP ([^{18}F]**3)** could be efficiently labeled within 90 min with good enantiomeric purity (>95%), good yield (11–37%) and high specific activity (21–69 GBq/μmol). Cell uptake studies showed FEP had higher uptake than FPP as well as reference ligand FET ([^{18}F]**1**). Uptake mechanism studies suggested that FEP is a selective substrate for system L and prefers its subtype LAT1. In vivo biodistribution studies demonstrated FEP had specific accumulation in tumor cells and tumor to background ratio reached 1.45 at 60 min. Small animal PET imaging studies showed FEP was comparable to FET for imaging rats bearing 9L tumor model. FEP had high uptake in 9L tumor compared to surrounding tissue and was quickly excreted through urinary tract.

Conclusion—Biological evaluations indicate that FEP ([^{18}F]**2**) is a potential useful tracer for tumor imaging with PET.

Keywords

^{18}F; Phenylalanine derivatives; PET; LATs; Imaging agent

CORRESPONDING AUTHOR ADDRESS: Hank F. Kung, Ph.D., Department of Radiology, University of Pennsylvania, 3700 Market Street, Room 305, Philadelphia, PA 19104. Tel: (215) 662-3096, Fax: (215) 349-5035; kunghf@gmail.com.

1. Introduction

Malignant tumors can be detected by imaging their increased metabolic rates for glucose, lipids and amino acids [1]. One interesting metabolic process as a target for metabolic tumor imaging is increased protein metabolism in proliferating cancer cells. Avid uptake of amino acids is a normal feature of rapidly proliferating cells [2]. A number of radiolabeled amino acids (Fig. 1) were developed and have established role in clinical applications, especially in brain tumor imaging [3,4]. Amino acid based tracers could overcome certain limitations of most commonly used 2-[^{18}F]fluoro-2-deoxy-D-glucose (FDG), namely high accumulation in inflammatory tissues and high uptake in normal brain tissues [4].

Uncontrolled and accelerated growth of cancer cells lead to elevated rate of protein synthesis and increased uptake of amino acids as energy source as well as carbon and nitrogen source in the synthesis of nucleotides, amino sugars et al [5]. Some natural amino acid based tracers such as [^{11}C]methionine (MET) and [^{11}C]tyrosine (TYR), their uptake reflects transport, protein synthesis and non-protein metabolic pathways such as transamination and transmethylation, which makes imaging kinetic analysis difficult [6–8]. While uptake of non-natural amino acids such as *O*-(2-[^{18}F]fluoroethyl)-L-tyrosine (FET, [^{18}F]**1**) [9], 3-[^{18}F]fluoro-αmethyl-L-tyrosine (FMT) [10], anti-1-amino-3-[^{18}F]fluoro-cyclobutyl-1-carboxylic acid (FACBC) [11], 3-[^{123}I]-α-methyl-L-tyrosine (IMT) [12] represents mainly transport activity but not protein synthesis. It appears that their differences in protein metabolism do not translate into difference in clinical applicability[3]. Moreover, ^{18}F ($t_{1/2}$ = 109.8 min) and ^{123}I ($t_{1/2}$ = 13.2 h) labeled non-natural amino acid derivatives have advantage of longer half-life than ^{11}C ($t_{1/2}$ = 20.2 min) and are generally more stable in vivo which simplifies image analysis [3,4,13]. For these reason, non-natural amino acids have been a main focus in current development of amino acid tracers [3,14,15].

Amino acids are taken up into cells mainly through specific membrane associated carrier proteins. Increased uptake of amino acids is mediated through increased expression and activity of amino acid transporters. Amino acid transporters identified so far are solute carrier transporters (SLC), which are classified into a number of transporter systems based on their sodium dependence, substrate specificity, kinetics, regulatory properties and sensitivity to pH and specific inhibitors [16]. Most commonly existing amino acid transporter systems in mammalian cells responsible for transporting neutral amino acids are system A (alanine preferring), ASC (alanine-serine-cystine preferring) and system L (leucine preferring) [17]. Sodium-independent amino acid transport system L (LATs), which is a major route for transporting large branched and aromatic amino acids has attracted special interest [18]. Studies demonstrated that system L is a promising target for developing PET tumor imaging agents [3,4,19]. The broad substrate selectivity of LATs enables it to transport amino acid-related compounds. A number of substrates of LATs, such as MET, FET, FACBC, IMT, are clinically utilized for imaging brain cancer, head and neck cancer, lung cancer and prostate cancer et al [3,4,15]. System L is commonly upregulated in many tumors and correlated with tumor growth and prognosis [19–21]. There are four subtypes of LATs identified and characterized in molecular level, designated LAT1 to LAT4 [22]. In particular, LAT1 is most studied. LAT1 is primarily expressed in brain, placenta and tumors and closely correlated with angiogenesis [23], cell proliferation [23] and prognosis of patients with astrocytoma [24], non-small cell lung cancer (NSCLC) [25] and prostate cancer [26].

Phenylalanine and tyrosine derivatives, which are primarily LATs substrate, have proven to be useful tumor imaging agents [3,4]. In particular, FET ([^{18}F]**1)** is one of the first ^{18}F labeled amino acid tracers that could be prepared in large quantity for clinical use and satellite distribution similar to FDG [27]. FET is useful for detecting brain tumors and head

and neck squamous carcinoma, but its applications in peripheral tumors are somewhat limited [28,29]. Another clinically utilized system L substrate *p*-[^{123}I]iodo-L-phenylalanine (IPA) demonstrated potential for imaging brain tumor as well [30]. This led us to develop its fluoroalkyl derivatives, which are also structural analogs of FET. Our goal is to develop new amino acid tracers with improved in vivo pharmacokinetics than FET, which could lead to a higher tumor uptake and/or lower urinary excretion that may be beneficial for imaging tumors in urinary tract such as prostate cancer, urinary bladder carcinomas and cervical cancer [31,32]. Eliminating oxygen to form direct linkage of fluoroalkyl chain to phenyl ring provides a way to alter ligands' lipophilicity as well as to reduce length of side chain. In this study, we describe the synthesis, radiolabeling and biological evaluation of two new phenylalanine derivatives, *p*-(2-[^{18}F]fluoroethyl)-L-phenylalanine (FEP, [^{18}F]**2**) and *p*-(3-[^{18}F]fluoropropyl)-L-phenylalanine (FPP, [^{18}F]**3**) (Fig. 2). Clinically utilized FET ([^{18}F]**1**) was used as reference in biological evaluation of new ligands.

2. Materials and methods

2.1. General

All chemicals were purchased from Aldrich Chemical (St. Louis, MO) or TCI America (Portland, OR). The commercially available materials were used without further purification unless otherwise indicated. ^{1}H spectra and ^{13}C NMR was recorded by a Bruker DPX spectrometer at 200 MHz and 50 MHz respectively and referenced to NMR solvents as indicated. Chemical shifts are reported in ppm (δ), coupling constant *J* in Hz. High-resolution mass spectrometry (HRMS) data were obtained with an Agilent (Santa Clara, CA) G3250AA LC/MSD TOF system. Thin-layer chromatography (TLC) analyses were performed using Merck (Whitehouse Station, NJ) silica gel 60 F_{254} plates. Crude compounds generally were purified by flash column chromatography (FC) packed with silica gel (Aldrich). [^{18}F]Fluoride was purchased from IBA Molecular (Somerset, NJ) as an [^{18}O]enriched aqueous solution of [^{18}F]fluoride. Solid-phase extraction (SPE) cartridges such as Sep-Pak QMA Light and Oasis HLB cartridges were purchased from Waters (Milford, MA). High performance liquid chromatography (HPLC) was performed on an Agilent 1100 series system. [^{18}F]radioactivity was measured by gamma counter (Cobra II auto-gamma counter D5003 spectrometer, Canberra-Packard) in the 400–1600 keV energy range. Specific activity (SA) was calculated by comparing UV peak intensity of final products with calibration curves of corresponding non-radioactive standards of known concentrations. The animal experiments were carried out in compliance with ethics and animal welfare according to regulation requirements.

2.2. Chemistry

2.2.1. (S)-tert-butyl 2-(tert-butoxycarbonylamino)-3-(4-hydroxyphenyl)propanoate (5)—L-tyrosine *tert*-butyl ester (**4**, 949 mg, 4 mmol) was added to a round-bottom flask and dissolved in 40 mL MeOH/H_2O (2:1). To this mixture was added $NaHCO_3$ (1.008 g, 12 mmol) followed by Boc_2O (1.31 g, 6 mmol). The reaction mixture was allowed to stir for 4 h until completion as determined by TLC analysis (MeOH/CH_2Cl_2, 5/100). Upon completion, the mixture was concentrated under reduced pressure to remove methanol and then resulting solution diluted with water and extracted with EtOAc. Combined organic layer washed with brine and dried over Na_2SO_4, then concentrated under reduced pressure and purified by FC (MeOH/CH_2Cl_2, 5/100) to afford the product as white foam. ^{1}H NMR (200 MHz, $CDCl_3$) δ = 7.04 (d, 2H, *J* = 8.6 Hz), 6.75 (d, 2H, *J* = 8.6 Hz), 4.98 (d, 1H, *J* = 8.0 Hz), 4.43-4.36 (m, 1H), 2.98 (d, 2H, *J* = 5.8 Hz), 1.43 (s, 18H). ^{13}C NMR (50 MHz, $CDCl_3$) δ = 171.5, 155.6, 155.4, 130.8, 128.0, 115.6, 82.4, 55.4, 37.9, 28.5, 28.2. HRMS calcd for $C_{18}H_{27}NO_5$ ([M+Na]$^+$) 360.1997, found 360.1986. $[\alpha]^{24}_D$ +39.3° (c 0.29, $CHCl_3$).

2.2.2. (S)-tert-butyl2-(tert-butoxycarbonylamino)-3-(4-(trifluoromethylsulfonyloxy)phenyl)prop- anoate (6)—5 (515 mg, 1.53 mmol) and pyridine (302 mg, 3.82 mmol) in CH_2Cl_2 at 0 °C was added Tf_2O (385 μL, 2.29 mmol) dropwise. Reaction stirred for 45 min at 0 °C. Then dilute with CH_2Cl_2 (50 mL), washed with 1 N NaOH (5 mL), 10% citric acid (5 mL) and brine (10 mL). The organic layer was dried over $MgSO_4$, filtered and concentrated in vacuo. The residue was purified by FC (EtOAC/Hexanes, 1/9) to give **5** as light yellow liquid. ^{1}H NMR (200 MHz, $CDCl_3$) δ = 7.28 (d, 2H, *J* = 8.8 Hz), 7.19 (d, 2H, *J* = 9.0 Hz), 5.07 (d, 1H, *J* = 7.2 Hz), 4.53-4.37 (m, 1H), 3.07 (d, 2H, *J* = 6.0 Hz), 1.42 (s, 9H), 1.38 (s, 9H). ^{13}C NMR (50 MHz, MeOD) δ = 172.7, 157.9, 150.1, 140.0, 132.7, 122.4, 83.1, 80.8, 57.02, 38.4, 28.8, 28.3. HRMS calcd for $C_{19}H_{26}F_3NO_7S$ ($[M+Na]^+$) 492.1280, found 492.1299. $[\alpha]^{24}_D$ +28.7° (c 1.0, $CHCl_3$).

2.2.3. Stille cross-coupling for synthesis of 7a and 7b—Triflate **6** (1.0 equiv) in DMF was added to flamed dried flask containing LiCl (3.0 eqiv), $Pd(PPh_3)_2Cl_2$ (0.05 equiv), tributyl(vinyl)tin or tributyl(allyl)tin (1.3 equiv) in DMF. Reaction mixture was degassed for 5 min and then heated at 70 °C for 90 min at which point TLC indicated completion of reaction. The mixture was cooled to room temperature, diluted with water and then extracted three times with ether, combined organic layer was washed with brine, dried over $MgSO_4$, filtered and concentrated. Crude products were purified by FC (EtOAc/Hexanes, 5/95) to afford products as white solids.

2.2.3.1 (S)-tert-butyl 2-(tert-butoxycarbonylamino)-3-(4-vinylphenyl)propanoate (7a): Yield: 92%. ^{1}H NMR (200 MHz, $CDCl_3$) δ = 7.34 (d, 2H, *J* = 8.0 Hz), 7.14 (d, 2H, *J* = 8.2 Hz), 6.70 (dd, 1H, *J* = 17.6, 10.8 Hz), 5.73 (d, 1H, *J* = 17.6 Hz), 5.23 (d, 1H, *J* =10.8 Hz), 4.99 (d, 1H, *J* = 7.8 Hz), 4.54-4.37 (m, 1H), 3.05 (d, 2H, *J* = 6.0 Hz), 1.43 (s, 18H). ^{13}C NMR (50 MHz, $CDCl_3$) δ = 171.1, 155.3, 136.8, 136.5, 136.3, 129.9, 126.4, 113.7, 82.3, 79.9, 55.1, 38.5, 28.5, 28.2. HRMS calcd for $C_{20}H_{29}NO_4$ ($[M+Na]^+$) 370.1994, found 370.2001. $[\alpha]^{24}_D$ +42.7° (c 1.13, $CHCl_3$).

2.2.3.2 (S)-tert-butyl 2-(tert-butoxycarbonylamino)-3-(4-allylphenyl)propanoate(7b): Yield: 95%. ^{1}H NMR (200 MHz, $CDCl_3$) δ = 7.20-7.10 (m, 4H), 6.06-5.85 (m, 1H), 5.10 (d, 1H, *J* = 5.8 Hz), 5.05-4.96 (m, 2H), 4.54-4.37 (m, 1H), 3.36 (d, 2H, *J* = 6.8 Hz) 3.02 (d, 2H, *J* = 6.0 Hz), 1.43 (s, 18H). ^{13}C NMR (50 MHz, $CDCl_3$) δ =171.1, 155.2, 138.7, 137.6, 134.2, 129.7, 128.7, 115.8, 82.0, 79.7, 55.1, 40.0, 38.3, 28.5, 28.1. HRMS calcd for $C_{21}H_{31}NO_4$ ($[M+Na]^+$) 384.2151, found 384.2133. $[\alpha]^{24}_D$ +33.7° (c 0.47, $CHCl_3$).

2.2.4. Hydroboration-oxidation reaction for synthesis of 8a and 8b—To solution of corresponding alkene **7a** or **7b** in THF, 0.5 M 9-BBN in THF (3.0 equiv) was added dropwise, stirred for 3 h at room temperature. The solution was then cooled to 0 °C, 3 N NaOH solution was added followed by H_2O_2 (30% in H_2O). Reaction continued at room temperature for additional 3 h, the biphasic mixture was treated with saturated $Na_2S_2O_3$ and extract three times with EtOAc, combined organic extracts were washed with brine, dried over $MgSO_4$, filtered and concentrated. The crude mixtures were purified with FC (EtOAc/Hexanes, 3/7) to give products as clear viscous liquids.

2.2.4.1. (S)-tert-butyl 2-(tert-butoxycarbonylamino)-3-(4-(2-hydroxyethyl)phenyl)propanoate (8a): Yield: 86%. ^{1}H NMR (200 MHz, $CDCl_3$) δ = 7.20-7.08 (m, 4H), 4.99 (d, 1H, *J* = 6.8 Hz), 4.52-4.37 (m, 1H), 3,85 (t, 2H, *J* = 6.6 Hz), 2.98 (d, 2H, *J* = 5.8 Hz), 2.85 (t, 2H, *J* = 6.6 Hz), 1.42 (s, 18H). ^{13}C NMR (50 MHz, $CDCl_3$) δ = 171.1, 155.2, 137.3, 134.4, 129.7, 129.0, 82.0, 79.7, 63.6, 55.0, 38.9, 38.2, 28.3, 28.0. HRMS calcd for $C_{20}H_{31}NO_5$ ($[M+H]^+$) 366.2280, found 366.2281. $[\alpha]^{21}_D$ +41.4° (c 0.75, $CHCl_3$).

2.2.4.2. (S)-tert-butyl 2-(tert-butoxycarbonylamino)-3-(4-(2-hydroxypropyl)phenyl)propanoate (8b): Yield: 88%. ^{1}H NMR (200 MHz, $CDCl_3$) δ = 7.15-7.06 (m, 4H), 5.00 (d, 1H, *J* = 7.8 Hz), 4.49-4.37 (m, 1H), 3.67 (t, 2H, *J* = 6.4 Hz), 3.01 (d, 2H, *J* = 5.8 Hz), 2.68 (t, 2H, *J* = 6.6 Hz), 1.94-1.83 (m, 2H), 1.42 (s, 18H). ^{13}C NMR (50 MHz, $CDCl_3$) δ = 171.2, 155.3, 140.6, 134.0, 129.7, 128.6, 82.1, 79.9, 63.3, 55.1, 38.4, 34.4, 31.9, 28.5, 28.2. HRMS calcd for $C_{21}H_{33}NO_5$ ($[M+Na]^+$) 402.2256, found 402.2410. $[\alpha]^{24}_D$ +30.7° (c 0.93, $CHCl_3$).

2.2.5. Tosylation reaction for synthesis of precusors 9a and 9b—Corresponding hydroxyl compounds **8a or 8b** (1.0 equiv) in 5 mL CH_2Cl_2 was added Et_3N (3.0 equiv) and TsCl (1.2 equiv). Reaction continued at room temperature for 20 h. The solution was diluted with CH_2Cl_2, washed with saturated $NaHCO_3$ and brine. Orangic layer was dried over $MgSO_4$, filtered and concentrated. Purify via FC (EtOAc/Hexanes, 2/8) to afford products as clear viscous liquid.

2.2.5.1. (S)-tert-butyl 2-(tert-butoxycarbonylamino)-3-(4-(2-(tosyloxy)ethyl)phenyl)propanoate (9a): Yield: 92%. ^{1}H NMR (200 MHz, $CDCl_3$) δ = 7.72 (d, 2H, *J* = 8.2 Hz), 7.31 (d, 2H, *J* = 8.0 Hz), 7.11-7.00 (m, 4H), 4.97 (d, 1H, *J* = 7.8 Hz), 4.48-4.36 (m, 1H), 4.19 (t, 2H, *J* = 7.2 Hz), 3.02 (d, 2H, *J* = 5.6 Hz), 2.93 (t, 2H, J = 7.2 Hz), 2.45 (s, 3H), 1.43 (s, 18H). ^{13}C NMR (50 MHz, $CDCl_3$) δ = 171.0, 155.2, 144.8, 135.3, 134.9, 133.4, 130.0, 129.0, 128.0, 82.2, 79.9, 70.6, 55.0, 38.3, 35.2, 28.5, 28.1, 21.8. HRMS calcd for $C_{27}H_{37}NO_7S$ ($[M+Na]^+$) 542.2188, found 542.2221. $[\alpha]^{23}_D$ +28.0° (c 1.35, $CHCl_3$).

2.2.5.2. (S)-tert-butyl 2-(tert-butoxycarbonylamino)-3- (4-(2-(tosyloxy)propyl)phenyl)propan-oate (9b): Yield: 75%. ^{1}H NMR (200 MHz, $CDCl_3$) δ = 7.79 (d, 2H, *J* = 8.2 Hz), 7.35 (d, 2H, *J* = 8.0 Hz), 7.08-6.97 (m, 4H), 4.98 (d, 1H, *J* = 7.6 Hz), 4.48-4.36 (m, 1H), 4.03 (t, 2H, *J* = 6.2 Hz), 3.00 (d, 2H, *J* = 5.6 Hz), 2.61 (t, 2H, *J* = 7.8 Hz), 2.46 (s, 3H), 2.02-1.85 (m, 2H), 1.42 (s, 18H). ^{13}C NMR (50 MHz, $CDCl_3$) δ = 171.0, 155.2, 144.9, 139.1, 134.5, 133.5, 130.0, 129.8, 128.6, 128.1, 82.2, 79.9, 69.8, 55.1, 38.4, 31.3, 30.7, 28.5, 28.2, 21.8. HRMS calcd for $C_{28}H_{39}NO_7S$ ($[M+H]^+$) 534.2525, found 534.2518. $[\alpha]^{22}_D$ +29.5° (c 0.40, $CHCl_3$).

2.2.6. Fluorination for synthesis of 10a and 10b—Corresponding tosylate **9a** and **9b** (1.0 equiv) in 5 mL acetone was added sodium iodide (5.0 equiv). The reaction mixture was refluxed for 1 h and then filtered and concentrated. Residue was dissolved in CH_2Cl_2, filtered and concentrated again to afford clear liquid. This intermediate product was redissolved in CH_3CN, silver fluoride (4.0 mmol) was added in the solution and reaction continued at room temperature for 1 d at dark. Reaction mixture was then filtered and concentrated, purified with FC to afford products as light yellow viscous liquids.

2.2.6.1. (S)-tert-butyl 2-(tert-butoxycarbonylamino)-3-(4-(2-fluoroethyl)phenyl)propanoate (10a): Yield: 50%. ^{1}H NMR (200 MHz, $CDCl_3$) δ = 7.18-7.05 (m, 4H), 4.99 (d, 1H, *J* = 7.8 Hz), 4.73 (t, 1H, 6.6 Hz), 4.53-4.35 (m, 2H), 3.10-3.00 (m, 3H), 2.93 (t, 1H, *J* = 6.6 Hz), 1.42 (s, 18H). ^{13}C NMR (50 MHz, $CDCl_3$) δ = 171.2, 155.3, 135.9, 135.1, 130.0, 129.2, 84.2 (d, *J* = 168.5 Hz), 82.2, 55.1, 38.5, 36.8 (d, *J* = 20.0 Hz), 28.5, 28.2. HRMS calcd for $C_{20}H_{30}FNO_4$ ($[M+Na]^+$) 390.2057, found 390.2063. $[\alpha]^{23}_D$ +38.0° (c 0.45, $CHCl_3$).

2.2.6.2. (S)-tert-butyl 2-(tert-butoxycarbonylamino)-3-(4-(2-fluoropropyl)phenyl)propanoate (10b): Yield: 58%. ^{1}H NMR (200 MHz, $CDCl_3$) δ = 7.20-7.07 (m, 4H), 4.98 (d, 1H, *J* = 8.0 Hz), 4.57 (t, 1H, 6.0 Hz), 4.48-4.30 (m, 2H), 3.02 (d,

2H, *J* = 5.8 Hz), 2.72 (t, 1H, *J* = 7.6 Hz), 2.12-1.96 (m, 2H), 1.43 (s, 18H). ^{13}C NMR (50 MHz, $CDCl_3$) δ = 171.2, 155.3, 139.8, 134.3, 129.9, 128.7, 83.3 (d, *J* = 164.0 Hz), 82.2, 79.9, 55.1, 38.4, 32.2 (d, *J* = 20.0 Hz), 31.1, 28.5, 28.2. HRMS calcd for $C_{21}H_{32}FNO_4$ ([M +Na]$^+$) 404.2213, found 404.2242. $[\alpha]^{24}_D$ +36.2° (c 1.4, $CHCl_3$).

2.2.7. Deprotection reaction for synthesis of 2 and 3—Corresponding protected compound **10a** and **10b** (1.0 equiv) in CH_2Cl_2 was added trifluoroacetic acid (TFA), stirred for 2 h to 4h at which point TLC indicated completion of reaction. Reaction mixture was concentrated in vacuo and residue was then dissolved in 2 mL methanol, adjust pH to 6–7 with 5% NH_4OH at which point white precipitate formed. The mixture was refrigerated overnight and then subjected to filtration, the solid was washed with methanol and dried in vacuo to afford products as white solids.

2.2.7.1. (S)-2-amino-3-(4-(2-fluoroethyl)phenyl)propanoic acid (2): Yield: 81%. ^{1}H NMR (200 MHz, MeOD+TFA-D) δ = 7.17-7.05 (m, 4H), 4.58 (dt, 2H, *J* = 47.2, 6.2 Hz), 4.21 (dd, 1H, *J* = 7.6, 5.4 Hz), 3.35-3.08 (m, 2H), 2.97 (dt, 2H, *J* = 24.6, 6.2 Hz). ^{13}C NMR (50 MHz, D_2O+DCl) δ = 171.0, 137.6, 132.1, 129.6, 85.1 (d, *J* = 156 Hz), 53.98, 35.6 (d, *J* = 19.5 Hz), 29.7. HRMS calcd for $C_{11}H_{14}FNO_2$ ([M+H]$^+$) 212.1087, found 212.1086. $[\alpha]^{23}_D$ −5.8° (c 0.75, 6N HCl).

2.2.7.2. (S)-2-amino-3-(4-(2-fluoropropyl)phenyl)propanoic acid (3): Yield: 64%. ^{1}H NMR (200 MHz, D_2O+DCl) δ = 6.79-6.69 (m, 4H), 4.09 (t, 1H, *J* = 6.0 Hz), 3.90-3.80 (m, 2H), 2.73(ddd, 2H, *J* = 14.6, 5.8, 7.6 Hz), 2.19 (t, 2H, *J* = 7.6 Hz), 1.59-1.31 (m, 2H). ^{13}C NMR (50 MHz, D_2O+DCl) δ = 172.0, 142.5, 132.3, 130.5,130.2, 85.7 (d, *J* = 156.5 Hz), 55.0, 36.1, 32.1 (d, *J* = 19.0 Hz), 31.2. HRMS calcd for $C_{12}H_{16}FNO_2$ ([M+H]$^+$) 226.1243, found 226.1256. $[\alpha]^{24}_D$ −5.7° (c 0.45, 6N HCl).

2.3. Radiosynthesis of FEP([^{18}F]2) and FPP ([^{18}F]3)

[^{18}F]Fluoride trapped a Sep-Pak light QMA cartridge (pre-conditioned with 10 mL 1 N $NaHCO_3$, 10 mL water and dried with N_2) was eluted with 0.6 mL tetrabutylammonium bicarbonate ($TBAHCO_3$) solution (21.5 mg $TBAHCO_3$ in 0.3 mL CH_3CN and 0.3 mL H_2O). The ^{18}F activity was dried azeotropically under N_2 at 110 °C. Precursor **9a** or **9b** (5 mg) in 1 mL anhydrous CH_3CN was then added into dried ^{18}F, fluorination reaction continued for 5 min at 80 °C. After fluorination, reaction mixture was injected to semi-preparative HPLC on Phenomenex Gemini C-18 column (10 × 250 mm, 5 μm). Intermediates [^{18}F]**10a** and [^{18}F]**10b** were eluted with methanol/0.1% formic acid in water (80/20). Radioactive peak between 11 min to 13 min was collected and then diluted with 20–25 mL water, loaded on HLB oasis cartridge (preconditioned with 10 mL ethanol and 10 mL water), washed with 2 mL water and then eluted with 1 mL ethanol. Removing ethanol under N_2 at 60 °C. TFA was then added, deprotection reaction continued at 60 °C for 10 min. After removing TFA with N_2 flow, 1 mL sterile water was added to formulate final product. Chemical and radiochemical purity (RCP) were determined by analytical HPLC performed on a Phenomenex Gemini C-18 column (4.6 × 250 mm, 5 μm) eluted by solvent system A: methanol/0.1% formic acid (20/80) at flow rate of 1 mL/min and TLC (NH_4OH/ $MeOH/CH_2Cl_2$, 1/6/14). Retention time was 6.9 min for [^{18}F]**2** and 7.6 min for [^{18}F]**3**. Enantiomeric purity was determined with a chirobiotic-T (Aldrich, St. Louis, MO) chiral column (5 μ, 250 × 4.6 mm) using solvent system B: ethanol/H_2O (50/50) at flow rate of 0.5 mL/min. Retention time was 9.7 min for [^{18}F]**2** and 10.6 min for [^{18}F]**3**.

2.4. In vitro cell uptake studies and uptake mechanism studies in 9L cells

Brain gliosarcoma cell line 9L was purchased from ATCC (Manassas, VA). The 9L cells were cultured in Dulbecco's Modified Eagle's Medium (DMEM, GIBCO BRL, Grand

Island, NY) supplemented with 10% fetal bovine serum (Hycolne, Logan, UT) and 1% penicillin/streptomycin. Cells were maintained in T-75 culture flask under humidified incubator conditions (37 °C, 5% CO_2) and were routinely passaged at confluence. Tumor cells were plated at a concentration of 2.0×10^5 cells/well 24 h in culturing media prior to cell uptake and inhibition studies. On the day of experiment, the media was aspirated and the cells were washed three times with 1 mL of warm phosphate buffered saline (PBS, containing 0.90 mM of Ca^{2+} and 1.05 mM of Mg^{2+}). Each assay condition was performed in triplicates.

For cell uptake studies, ligand of choice was mixed within PBS solution and was then added to each well (~500,000 cpm/mL/well). The cells were incubated at 37 °C for 5, 30, 60, 120 min. At the end of the incubation period, the wells were aspirated free of ligand and then the residual cells were washed 3 times with 1 mL ice cold PBS without Ca^{2+} and Mg^{2+}. After washing with ice cold PBS, 350 μL 1 M NaOH was used to lyse the cells. The lysed cells were collected onto filter paper and counted using a gamma counter (Packard Cobra). Together with the sample of initial dose. 100 μL of the cell lysate was used for determination of protein concentration by Lowry method. The data was normalized as percentage uptake of initial dose relative to 100 μg protein content (% ID/100 μg protein).

In inhibition studies, [^{18}F]**2** was mixed with specific inhibitors in concentration of 0.5 mM, 1 mM and 5 mM in PBS solution. In sodium dependence studies, PBS buffer was replaced with Na^+ free solution (143 mM choline chloride, 2.68 mM KCl and 1.47 mM KH_2PO_4). The cells were incubated at 37 °C for 30 min. The procedure following incubation was the same as in cell uptake studies. The data was normalized in reference to uptake of [^{18}F]**2** without any inhibitor in PBS solution.

2.5. In vivo Biodistribution in Fisher rats with 9L glioma tumors

F344 rats were purchased from Charles Rivers Laboratory (Malvern, PA). Xenografts using 9L cells in F344 rats were accomplished by injecting 4–5 million cells/xenograft. The cells suspended in PBS solution (0.2 mL) were injected subcutaneously into each of shoulder flanks of the F344 rat. The growth of the tumor was monitored daily for two weeks. When the volume of the tumors reached 1 cm, the rat tumor model was used for biodistribution or microPET imaging studies. Animals were fasted for 12–18 hours prior to the procedure. Saline solution containing the radioactive compounds in a small volume (0.2 mL) was injected into the lateral tail vein under isoflurane anesthesia (1–2%, 1 L/min oxygen). The animals were sacrificed at 30 and 60 min time points post-injection by cardiac excision under anesthesia. Six rats were sacrificed at each time point. The organs of interest and tumors were removed and weighed. The radioactivity in each tissue was measured using gamma counter together with sample of the initial dose. Results were expressed as the percentage of the injected dose per gram (%ID/g) of tissue. Each value represents the mean ± SD of six rats unless otherwise noted.

2.6. Small animal imaging with a microPET

PET imaging studies were performed on a Phillips Mosaic small animal PET scanner, which has an imaging field of view of 11.5 cm. Under isoflurane anesthesia (1–2%, 1L/min oxygen) the tumor bearing F344 rats as described before were injected with 30–37 MBq (0.8–1 mCi) of activity via an intravenous injection into the lateral tail vein. Data acquisition began immediately following the intravenous injection. Dynamic scans were conducted over a period of 2 h (5 min/frame; image voxel size 0.5 mm^3). Rats were visually monitored for breathing and a heating pad was used to maintain body temperature throughout the entire procedure. Images were reconstructed and region of interest (ROI) analysis was performed using AMIDE software (http://amide.sourceforge.net/).

3. Results and Discussion

3.1 Chemistry

An efficient synthesis of fluoroalkyl phenylalanine derivatives **2** and **3** was carried out as shown in Scheme 1. The tosylate precursors **9a** and **9b** for labeling could be prepared in five steps in an overall yield of 60 and 52% respectively starting from commercially available L-tyrosine *tert*-butyl ester. Standard Boc protection of amine group and then triflation of phenol group on protected tyrosine **5** afforded triflate **6** in 83% yield. Triflate **6** then underwent Stille cross-coupling reaction with vinyl or allyl tributylstanne and Pd catalyst $Pd(PPh_3)_2Cl_2$ in anhydrous DMF at 70 °C for 1 h to yield corresponding alkenes. Hydroboration alkenes **7a** or **7b** with 9-BBN and subsequent oxidation with sodium peroxide afforded aliphatic alcohol **8a** and **8b** in 86 to 88% yield. We chose 9-BBN as hydroboration reagent because of its high regio-selectivity in comparison to BH_3 reagent, initial reaction with BH_3·THF had low yield (< 20%). Tosylation of the alcohol compounds afforded labeling precursors in 75 to 92% yield. After a two-step fluorination – tosylate **9a** or **9b** was first convert to iodide by refluxing with sodium iodide in acetone and then fluorinated by reacting with silver fluoride, and deprotection with TFA, the standard **2** and **3** were obtained in an overall yield of 24% and 19% respectively. The enantiomeric purity of precursors and standards for radiolabeling is >95% analyzed by chiral HPLC.

3.2 Radiosynthesis of FEP([^{18}F]2) and FPP ([^{18}F]3)

Preparation of FEP ([^{18}F]**2**) and FPP ([^{18}F]**3**) was carried out via a two-step reaction as shown in Scheme 2. First step was no-carrier-added (NCA) nucleophilic fluorination with dried TBA^{18}F and $TBAHCO_3$ in acetonitrile. Intermediate [^{18}F]**10a** or [^{18}F]**10b** was then subjected to semi-preparative HPLC purification and HLB oasis solid phase extraction to eliminate unreacted ^{18}F fluoride and other by-products. Second step was to remove protecting groups using TFA at 60 °C. The results of labeling reactions were summarized in Table 1. Enantiomerically pure [^{18}F]**2** and [^{18}F]**3** could be prepared in 90 min with high radio purity (> 95% as measured by analytical HPLC and TLC), good yield (11 to 37%) and high specific activity (21 to 69 GBq/μmol) at the end of synthesis.

3.3 Cell uptake studies

At first, we compared the time dependent uptake of new ligands FEP ([^{18}F]**2**) and FPP ([^{18}F]**3**) to clinically utilized FET ([^{18}F]**1**) in 9L gliosarcoma cells (Fig. 3). Uptake of tracers was measured at selected time points up to 2 h. Three ligands demonstrated very similar kinetics, reaching maximum uptake within 60 min and then washed out. The uptake follows order FEP ([^{18}F]**2**)> FET ([^{18}F]**1**) ≈ FPP ([^{18}F]**3**). The maximum uptake of FEP is about 1.4 fold of FET. In vitro uptake studies showed FEP had a high accumulation and good retention in 9L glioma cells. The uptake results indicate that fluoroalkyl side chain may be more desirable for aromatic amino acid tracers. This agrees with the results reported by Tsukada et al, they found the shorter ^{18}F-fluoroalkyl chain length L-tyrosine provided a better tumor-to-blood ratio.[33] Based on the encouraging results reported in this paper, additional studies are warranted to further characterize this series of fluoroalkyl phenylalanine derivatives, [^{18}F]**1** and **2**.

3.4 Uptake mechanism studies of FEP ([^{18}F]2)

Uptake of amino acid based tracers depends on a group of amino acid transport systems, which often have substantial overlap in substrate selectivity and thus a single radiolabeled amino acid can be substrate for multiple amino acid transport systems. We are interested in characterizing the uptake mechanism of FEP ([^{18}F]**2**) into tumor cells. To achieve this goal, we conducted competitive uptake inhibition studies using inhibitors specific for system A,

ASC and L, given that transport of neutral amino acids into mammalian cells is predominantly via these systems [21]. The uptake of FEP ([^{18}F]**2**) was measure in absence of inhibitors as well as in the presence of concentration from 0.5 to 5 mM of *N*-methyl-α-aminoisobutyric acid (MeAIB), L-alanine (L-Ala), L-serine(L-Ser), 2-amino-bicylo[2.2.1]heptane-2-carboxylic acid (BCH), D-methionine and *N*-Ethylmaleimide (NEM). MeAIB is selective inhibitor of system A while L-Ala and L-Ser are inhibitors of system ASC. BCH is primarily an inhibitor for sodium independent system L but it is also an inhibitor for sodium dependent system B^0 and $B^{0,+}$ [17]. To measure the contribution from sodium dependent transport systems, we carried out sodium dependence studies comparing uptake in sodium-free buffer to uptake in PBS. To further explore the preference of FEP towards the subtypes of LATs, we carried out competitive inhibition studies using D-Met, specific inhibitor for LAT1 and *N*-ethylmaleimide (NEM), inhibitor for other subtypes LAT2 to LAT4 [22,34]. These studies were performed with a 30 min incubation time and the results were normalized to uptake of FEP in phosphate buffer solution (PBS) in absence of inhibitors as summarized in Fig. 4.

Uptake of FEP ([^{18}F]**2**) is sodium independent since replacing Na^+ with choline showed no difference. The effect of inhibition is concentration dependent. Uptake of FEP is most sensitive to inhibitor of LATs. 5 mM BCH can inhibit more than 98% of uptake. On the contrast, no inhibition was observed using MeAIB, which indicates system A has no contribution in uptake of FEP. Inhibition of ASC via L-Ala or L-Ser has some effect but not as significant as system L, maximum inhibition at 5 mM is about 90%. The results demonstrated that FEP ([^{18}F]**2**) was selective substrate for sodium independent transporter system L. Futhermore, LAT1 specific inhibitor D-Met has very similar effect as BCH. The impact of NEM on the uptake is much less compared to D-Met, the maximum inhibition at 5 mM is ~30%, this suggests uptake of FEP may prefer LAT1 in comparison to other subtypes of LATs. It is an interesting difference in comparison to previously reported FET ([^{18}F]**1)**, which is suggested to be selectively transported via LAT2. [27] There is some advantage targeting LAT1 because it plays a critical role in cell growth and proliferation and shows increased transport activity in many malignant tumors. [19,20] LAT1 expression is rarely detected in nontumor areas, in contrast, LAT2 is more ubiquitously expressed and has a high level of expression in small intestine, kidney, placenta, as well as tissues rich in (re)absorbing epithelia. [35] Some cancer cells such as C6 rat glioma, HeLa cervix carcinoma cells and R1M rhabdomyosarcoma have high expression of LAT1 but showed no upregulation of LAT2. [36,37] In such cancer cells lack of expression of LAT2, FEP ([^{18}F]**2**) might have advantage over FET ([^{18}F]**1**). Further investigations are needed to identify the amino acid transport systems involved in the uptake process.

3.5 in vivo biodistribution studies of FEP ([^{18}F]2)

From in vitro studies results, FEP seemed to be a potential tracer that worth further investigations, so in vivo evaluations were conducted. The in vivo biodistribution studies were carried out in fisher rats bearing 9L tumor model, which is a well-established animal model mimicking clinical glioblastoma multiform and a number of amino acid based tracers used this model for biological evaluations [11,38]. The distribution of radioactivity in selective peripheral tissues and organs and the regional radioactivity distribution in rat brain at 30 min and 60 min after injection of FEP were shown in Table 2.

The results showed FEP had higher accumulation in 9L tumor compared to surrounding organs and tissues. The tumor to brain and tumor to muscle ratio increased slightly from 30 to 60 min (from 1.55 to 1.73). Tumor to blood ratio increases from 1.12 at 30 min to 1.38 at 60 min. The highest uptake was found in the pancreas, accumulation in other organs is lower than that in tumor. Bone uptake is not significant, which indicates that FEP ([^{18}F]**2**) is metabolically stable. Similar to FET ([^{18}F]**1)** [38], FEP ([^{18}F]**2)** had high uptake in

pancreases. This is typical for labeled amino acid analog in rodents, which might due to high protein turnover in pancreas. Tumor uptake, bone uptake and tumor to muscle ratio is comparable to reported FET results in the same rat tumor model, but FEP seems to have slightly higher normal brain uptake compared with FET resulting lower tumor to brain ratio [38].

3.6 Small animal imaging studies

Finally, the in vivo tumor imaging in the rats bearing 9L model was examined. Small animal PET imaging studies in living rats were performed and time-activity curves were generated by drawing region of interest to assess the kinetics of FEP ([^{18}F]**2**) in comparison to FET ([^{18}F]**1**). FET and FEP exhibited very similar results as shown in Fig. 5. Both tracers have higher accumulations in tumors than surrounding background. After 20 min of intravenous injection of FEP, radioactivity in heart and muscle reached a plateau (Fig. 6). FEP had prolonged accumulation in 9L tumors with a slow steadily increase in 2 h imaging period. High urinary excretion was observed for both tracers, which is typical for tyrosine and phenylalanine analogs. Tumor to muscle ratio of these two ligands is comparable, which rapidly reached a plateau within 20 min (as shown in Fig. 7). Imaging results indicate FEP ([^{18}F]**2**) is compared to FET ([^{18}F]**1**), both are suitable for brain tumor imaging.

4. Conclusion

In summary, we prepared new optically pure phenylalanine derivatives FEP ([^{18}F]**2**) and FPP ([^{18}F]**3**) in high radiochemical purity, good radiochemical yield (11–37%) and high specific activity (21–69 GBq/μmol). Cellular uptake in 9L glioma demonstrated that FEP had a higher uptake than FPP and previously reported FET ([^{18}F]**1**). Uptake mechanism studies suggested that accumulation of FEP into 9L cells was predominantly via system L. In vivo biodistributon studies using rats bearing 9L glioma tumor model showed that FEP had higher uptake in 9L glioma than surrounding organs. Small animal PET imaging studies demonstrated that FEP was comparable to FET. These results indicate that FEP ([^{18}F]**2**) is a potential useful PET tumor imaging agent.

References

1. Plathow C, Weber WA. Tumor cell metabolism imaging. J Nucl Med. 2008; 49 (Suppl 2):43S–63S. [PubMed: 18523065]
2. van Waarde A, Elsinga PH. Proliferation markers for the differential diagnosis of tumor and inflammation. Curr Pharm Des. 2008; 14:3326–339. [PubMed: 19075707]
3. McConathy J, Goodman Mark M. Non-natural amino acids for tumor imaging using positron emission tomography and single photon emission computed tomography. Cancer metastasis reviews. 2008; 27:555–73. [PubMed: 18648909]
4. Jager PL, Vaalburg W, Pruim J, de Vries EG, Langen KJ, Piers DA. Radiolabeled amino acids: basic aspects and clinical applications in oncology. J Nucl Med. 2001; 42:432–45. [PubMed: 11337520]
5. Ganapathy V, Thangaraju M, Prasad PD. Nutrient transporters in cancer: Relevance to Warburg hypothesis and beyond. Pharmacol Ther. 2008
6. Fujibayashi Y, Kawai K, Yonekura Y, Matsumoto K, Konishi J, Yokoyama A. Problems of [S-methyl-11C]-L-methionine as a protein synthesis marker in the pancreas. Ann Nucl Med. 1990; 4:29–33. [PubMed: 2206769]
7. Ishiwata K, Enomoto K, Sasaki T, Elsinga PH, Senda M, Okazumi S, et al. A feasibility study on L-[1-carbon-11]tyrosine and L-[methyl-carbon-11]methionine to assess liver protein synthesis by PET. J Nucl Med. 1996; 37:279–85. [PubMed: 8667062]

8. Willemsen AT, van Waarde A, Paans AM, Pruim J, Luurtsema G, Go KG, et al. In vivo protein synthesis rate determination in primary or recurrent brain tumors using L-[1–11C]-tyrosine and PET. J Nucl Med. 1995; 36:411–9. [PubMed: 7884503]
9. Heiss P, Mayer S, Herz M, Wester HJ, Schwaiger M, Senekowitsch-Schmidtke R. Investigation of transport mechanism and uptake kinetics of O-(2-[18F]fluoroethyl)-L-tyrosine in vitro and in vivo. J Nucl Med. 1999; 40:1367–73. [PubMed: 10450690]
10. Inoue T, Tomiyoshi K, Higuichi T, Ahmed K, Sarwar M, Aoyagi K, et al. Biodistribution studies on L-3-[fluorine-18]fluoro-alpha-methyl tyrosine: a potential tumor-detecting agent. J Nucl Med. 1998; 39:663–7. [PubMed: 9544678]
11. Yu W, Williams L, Camp VM, Olson JJ, Goodman MM. Synthesis and biological evaluation of anti-1-amino-2-[18F]fluoro-cyclobutyl-1-carboxylic acid (anti-2-[18F]FACBC) in rat 9L gliosarcoma. Bioorg Med Chem Lett. 20:2140–3. [PubMed: 20207538]
12. Prante O, Deichen JT, Hocke C, Kuwert T. Characterization of uptake of 3-[(131)I]iodo-alpha-methyl-L-tyrosine in human monocyte-macrophages. Nucl Med Biol. 2004; 31:365–72. [PubMed: 15028249]
13. Couturier O, Luxen A, Chatal JF, Vuillez JP, Rigo P, Hustinx R. Fluorinated tracers for imaging cancer with positron emission tomography. Eur J Nucl Med Mol Imaging. 2004; 31:1182–206. [PubMed: 15241631]
14. Fowler JS, Ding YS, Volkow ND. Radiotracers for positron emission tomography imaging. Semin Nucl Med. 2003; 33:14–27. [PubMed: 12605354]
15. Laverman P, Boerman OC, Corstens FH, Oyen WJ. Fluorinated amino acids for tumour imaging with positron emission tomography. Eur J Nucl Med Mol Imaging. 2002; 29:681–90. [PubMed: 11976809]
16. Hyde R, Taylor PM, Hundal HS. Amino acid transporters: roles in amino acid sensing and signalling in animal cells. Biochem J. 2003; 373:1–18. [PubMed: 12879880]
17. Palacin M, Estevez R, Bertran J, Zorzano A. Molecular biology of mammalian plasma membrane amino acid transporters. Physiol Rev. 1998; 78:969–1054. [PubMed: 9790568]
18. Christensen HN. Role of amino acid transport and counter transport in nutrition and metabolism. Physiol Rev. 1990; 70:43–77. [PubMed: 2404290]
19. Yanagida O, Kanai Y, Chairoungdua A, Kim DK, Segawa H, Nii T, et al. Human L-type amino acid transporter 1 (LAT1): characterization of function and expression in tumor cell lines. Biochim Biophys Acta. 2001; 1514:291–302. [PubMed: 11557028]
20. Fuchs BC, Bode BP. Amino acid transporters ASCT2 and LAT1 in cancer: partners in crime? Semin Cancer Biol. 2005; 15:254–66. [PubMed: 15916903]
21. Saier MH Jr, Daniels GA, Boerner P, Lin J. Neutral amino acid transport systems in animal cells: potential targets of oncogene action and regulators of cellular growth. J Membr Biol. 1988; 104:1–20. [PubMed: 3054116]
22. Bodoy S, Martin L, Zorzano A, Palacin M, Estevez R, Bertran J. Identification of LAT4, a novel amino acid transporter with system L activity. J Biol Chem. 2005; 280:12002–11. [PubMed: 15659399]
23. Kaira K, Oriuchi N, Imai H, Shimizu K, Yanagitani N, Sunaga N, et al. l-type amino acid transporter 1 and CD98 expression in primary and metastatic sites of human neoplasms. Cancer Sci. 2008; 99:2380–6. [PubMed: 19018776]
24. Nawashiro H, Otani N, Shinomiya N, Fukui S, Ooigawa H, Shima K, et al. L-type amino acid transporter 1 as a potential molecular target in human astrocytic tumors. Int J Cancer. 2006; 119:484–92. [PubMed: 16496379]
25. Kaira K, Oriuchi N, Imai H, Shimizu K, Yanagitani N, Sunaga N, et al. Prognostic significance of L-type amino acid transporter 1 expression in resectable stage I–III nonsmall cell lung cancer. Br J Cancer. 2008; 98:742–8. [PubMed: 18253116]
26. Sakata T, Ferdous G, Tsuruta T, Satoh T, Baba S, Muto T, et al. L-type amino-acid transporter 1 as a novel biomarker for high-grade malignancy in prostate cancer. Pathol Int. 2009; 59:7–18. [PubMed: 19121087]

27. Langen KJ, Hamacher K, Weckesser M, Floeth F, Stoffels G, Bauer D, et al. O-(2-[18F]fluoroethyl)-L-tyrosine: uptake mechanisms and clinical applications. Nucl Med Biol. 2006; 33:287–94. [PubMed: 16631076]

28. Pauleit D, Stoffels G, Schaden W, Hamacher K, Bauer D, Tellmann L, et al. PET with O-(2–18F-Fluoroethyl)-L-Tyrosine in peripheral tumors: first clinical results. J Nucl Med. 2005; 46:411–6. [PubMed: 15750152]

29. Lau EW, Drummond KJ, Ware RE, Drummond E, Hogg A, Ryan G, et al. Comparative PET study using F-18 FET and F-18 FDG for the evaluation of patients with suspected brain tumour. J Clin Neurosci. 17:43–9. [PubMed: 20004582]

30. Hellwig D, Ketter R, Romeike BF, Sell N, Schaefer A, Moringlane JR, et al. Validation of brain tumour imaging with p-[123I]iodo-L-phenylalanine and SPECT. Eur J Nucl Med Mol Imaging. 2005; 32:1041–9. [PubMed: 15902439]

31. Shreve PD, Anzai Y, Wahl RL. Pitfalls in oncologic diagnosis with FDG PET imaging: physiologic and benign variants. Radiographics. 1999; 19:61–77. quiz 150-1. [PubMed: 9925392]

32. Ahlstrom H, Malmstrom PU, Letocha H, Andersson J, Langstrom B, Nilsson S. Positron emission tomography in the diagnosis and staging of urinary bladder cancer. Acta Radiol. 1996; 37:180–5. [PubMed: 8600958]

33. Tsukada H, Sato K, Fukumoto D, Kakiuchi T. Evaluation of D-isomers of O-F-18-fluoromethyl, O-F-18-fluoroethyl and O-F-18-fluoropropyl tyrosine as tumour imaging agents in mice. European Journal of Nuclear Medicine and Molecular Imaging. 2006; 33:1017–24. [PubMed: 16699766]

34. Tomi M, Mori M, Tachikawa M, Katayama K, Terasaki T, Hosoya K. L-type amino acid transporter 1-mediated L-leucine transport at the inner blood-retinal barrier. Invest Ophthalmol Vis Sci. 2005; 46:2522–30. [PubMed: 15980244]

35. Rossier G, Meier C, Bauch C, Summa V, Sordat B, Verrey F, et al. LAT2, a new basolateral 4F2hc/CD98-associated amino acid transporter of kidney and intestine. J Biol Chem. 1999; 274:34948–54. [PubMed: 10574970]

36. Kersemans V, Cornelissen B, Kersemans K, Bauwens M, Dierckx RA, De Spiegeleer B, et al. 123/125I-labelled 2-iodo-L: -phenylalanine and 2-iodo-D: -phenylalanine: comparative uptake in various tumour types and biodistribution in mice. Eur J Nucl Med Mol Imaging. 2006; 33:919–27. [PubMed: 16572305]

37. Urakami T, Sakai K, Asai T, Fukumoto D, Tsukada H, Oku N. Evaluation of O-[(18)F]fluoromethyl-D-tyrosine as a radiotracer for tumor imaging with positron emission tomography. Nucl Med Biol. 2009; 36:295–303. [PubMed: 19324275]

38. Lee TS, Ahn SH, Moon BS, Chun KS, Kang JH, Cheon GJ, et al. Comparison of 18F-FDG, 18F-FET and 18F-FLT for differentiation between tumor and inflammation in rats. Nucl Med Biol. 2009; 36:681–6. [PubMed: 19647174]

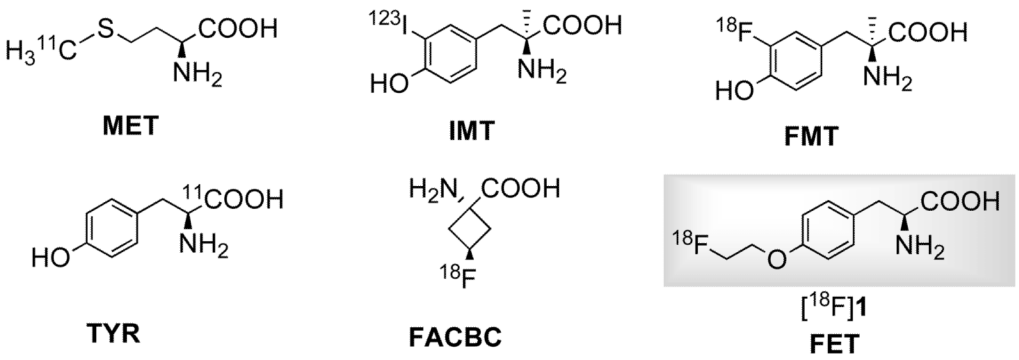

Fig. 1.
Some clinically utilized amino acid based tracers

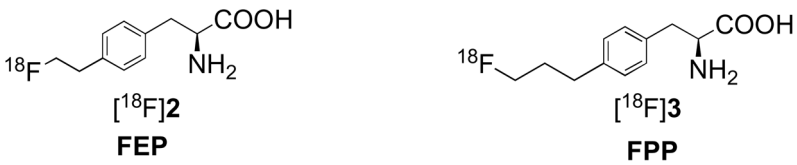

Fig. 2.
Chemical structures of new phenylalanine derivatives

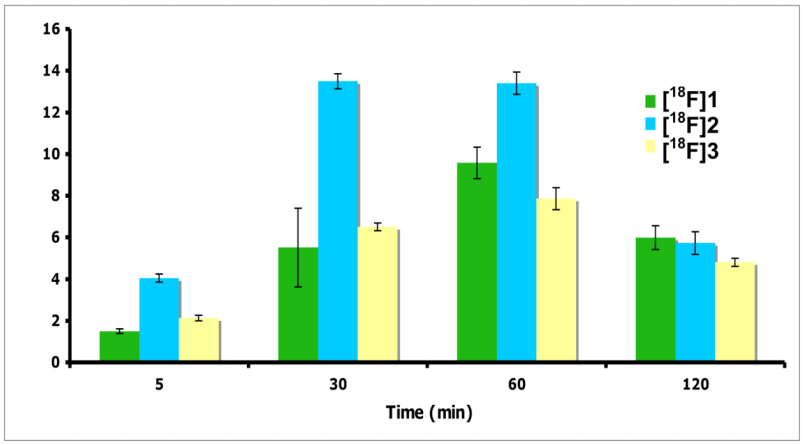

Fig. 3.

Time course of uptake of FET ([^{18}F]**1**), FEP ([^{18}F]**2**)and FPP ([^{18}F]**3**) in 9L glioma cells. The uptake value was represented as % uptake/100 ug protein, mean ± SD (n = 3).

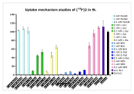

Fig. 4.

Summary of uptake mechanism studies of FEP ([^{18}F]**2**) in 9L glioma cells. Results were normalized to uptake of [^{18}F]**2** in PBS solution at 30 min. Data are expressed as mean ± SD (n = 3).

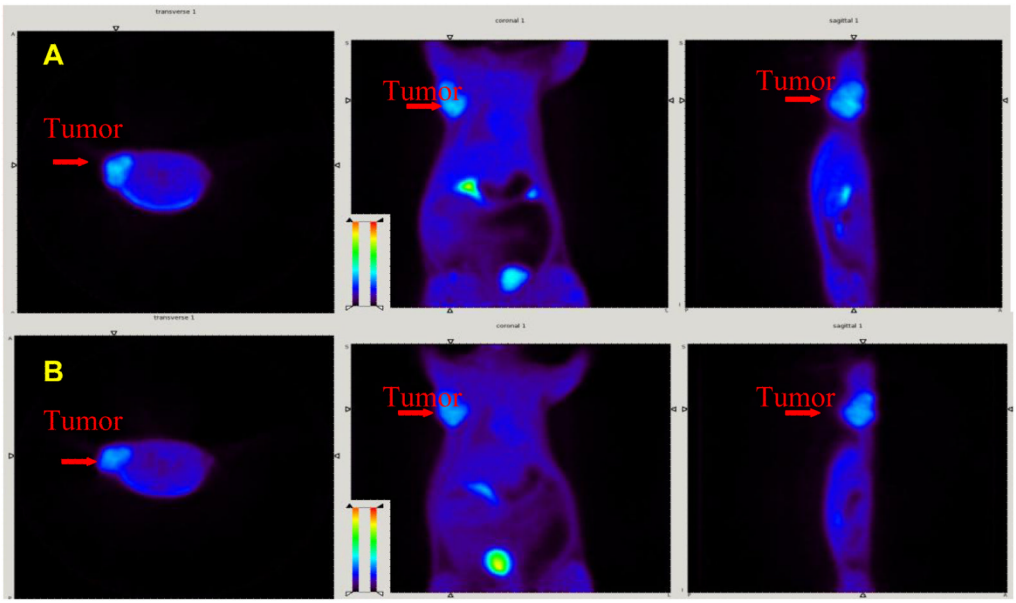

Fig. 5.

Small animal PET images of FEP ([^{18}F]**2**, A) and FET ([^{18}F]**1**, B) in tumor bearing rats. Color-coded PET images from summed 2 h data in transverse, coronal and sagital view from left to right followed injection of FEP and FET are shown. The arrowhead points to the 9L tumor.

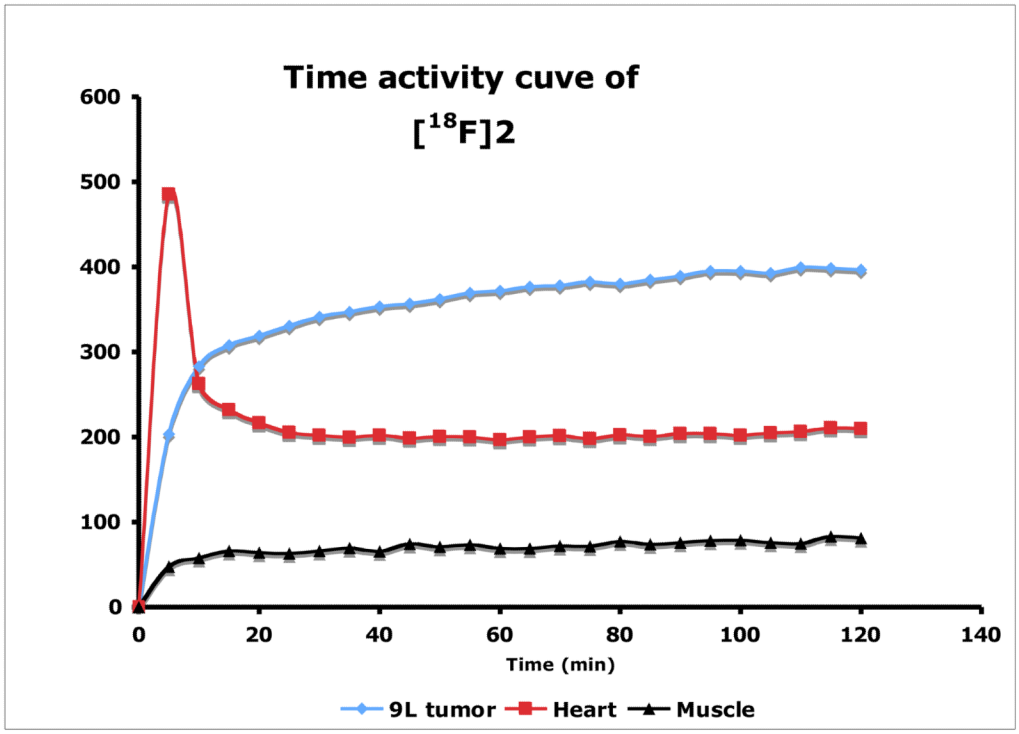

Fig. 6.
Time-Activity curve after injection of FEP ([^{18}F]**2**) in the rat.

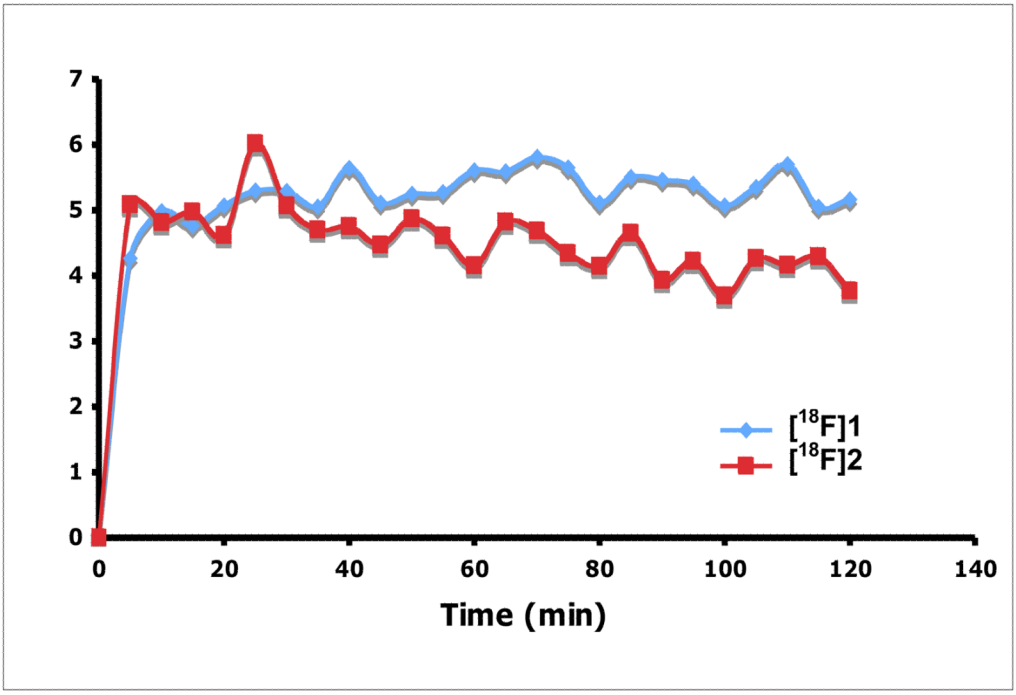

Fig. 7.
Comparison of FEP ([^{18}F]**2**) and FET ([^{18}F]**1**) tumor to muscle (T/M) ration.

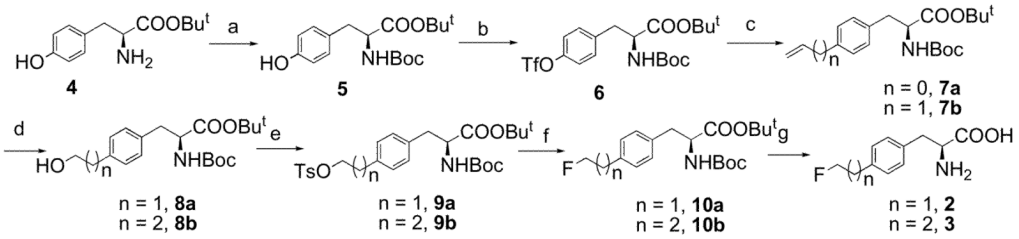

Scheme 1.

Synthesis of radiolabeling precursors and standards **2** and **3**. Reagents and Conditions: a) $(Boc)_2O$, $NaHCO_3$, MeOH, H_2O, rt, 89%; b) 2. Tf_2O, pyridine, CH_2Cl_2, 0°C, 93%; c) Tributyl vinyltin or tributyl allyltin, LiCl, $Pd(PPh_3)_2Cl_2$, DMF, 70°C, 92% (n = 0) or 95% (n = 1); d) 9-BBN, THF, NaOH, H_2O_2, 86% (n = 1) or 88% (n = 2); e) TsCl, Et_3N, CH_2Cl_2, 92% (n = 1) or 75% (n = 2); f) i. NaI, acetone, reflux; ii. AgF, CH_3CN, 50% (n = 1) or 58% (n = 2); g) TFA, CH_2Cl_2, 81% (n = 1) or 64% (n = 2).

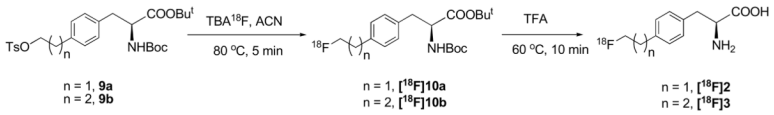

Scheme 2.
Radiolabeling of [^{18}F]FEP ([^{18}F]**2**) and [^{18}F]FPP ([^{18}F]**3**)

Table 1

Overall synthesis time, average decay-corrected yields (RCY), radiochemical purity (RCP), enantiomeric purity and specific activity at the end of synthesis.*

Ligands	Synthesis time (min)	RCY (%)	RCP (%)	Enantiomeric Purity (%)	Specific activity (GBq/μmol)
[^{18}F]**2**	75–82	27–37	> 95	> 95	31–69
[^{18}F]**3**	78–90	11–23	> 95	> 95	21–25

*Data obtained from two to six experiments.

Table 2

In vivo biodistribution of FEP ([^{18}F]**2**) in Fisher rats with 9L xenograft after single intravenous injection, reprented as % ID/g, mean ± SD (six rats per time point)

Organs	30 min	60 min
Blood	0.73 ± 0.08	0.65 ± 0.05
Heart	0.70 ± 0.07	0.63 ± 0.05
Muscle	0.58 ± 0.05	0.62 ± 0.05
Lung	0.68 ± 0.08	0.61 ± 0.05
Kidney	0.72 ± 0.05	0.63 ± 0.05
Pancreas	2.66 ± 0.20	2.45 ± 0.27
Spleen	0.75 ± 0.06	0.69 ± 0.05
Liver	0.71 ± 0.07	0.63 ± 0.05
Skin	0.57 ± 0.07	0.60 ± 0.09
Brain	0.53 ± 0.03	0.52 ± 0.05
Bone	0.41 ± 0.03	0.41 ± 0.04
Tumor *	0.82 ± 0.06	0.90 ± 0.20
Tumor/Brain	1.55	1.73
Tumor/Muscle	1.41	1.45

* Tumor n = 5 per time point.